

Highly-effective Integrated EMI Shields with Graphene and Nanomagnetic Multilayered Composites

Atom O. Watanabe, Junki Min,
Markondeya R. Pulugurtha,
and Rao R. Tummala
3D Systems Packaging Research Center
Georgia Institute of Technology
Atlanta, GA USA
email: atom@gatech.edu

Seungtaek Jeong, Subin Kim,
Youngwoo Kim, and Joungho Kim
Department of Electrical Engineering
Korea Advanced Institute
of Science and Technology
Daejeon, South Korea
email: seungtaek@kaist.ac.kr

Denny Wong and Ravi Mullanpudi
Tango Systems
San Jose, CA USA
email: dwong@tangosystems.com

Abstract—Electromagnetic interference (EMI) control is one of the most significant challenges for emerging consumer, automotive, Internet of things (IoT) and wearable systems. This paper demonstrates miniaturized and integrated nanostructures for component-level EMI isolation and external EMI shielding in ultra-miniaturized electronic systems. Multi-layered nanomagnetic and copper shielding materials are designed, synthesized, and characterized for their shielding effectiveness. Graphene is explored as an alternative EMI shield material. From the modeling and experimental analysis, the advantages of nanostructures for internal and external component-level shielding in different applications is discussed.

I. INTRODUCTION

With increased multi-functional integration and miniaturization of emerging consumer, IoT, and automotive electronics, component-level shielding has become extremely important to prevent undesired electromagnetic (EM) coupling [1], [2]. In automotive electronics, high-power modules in electric vehicles will require high switching frequencies greater than 10 MHz. In this frequency range, any unwanted noise coupling generated by direct current (DC)-DC converters can result in electromagnetic compatibility (EMC) issues [3]. In consumer electronics, the emerging trend in multi-mode multi-band (MMMB) systems such as in single module integration of a power amplifier (PA) and low-noise amplifier (LNA) creates noise coupling between the PA that acts as the aggressor and the LNA as the victim. EMC issues also arise from the near-field coupling between noise-prone logic integrated circuits (ICs) and noise-sensitive radio-frequency (RF) ICs [4].

EMI noise in traditional modules with large components is shielded by metallic cans and geometric isolation [5]. Shielding with conformal metal coatings of individual packaged components has also been demonstrated [2], [6]. Along with such conformal metal coatings on overmolded packages and dies, component-level shielding has been developed with integrated via-based shields inside packages [7], [8]. Such shielding is highly effective for isolating electric and magnetic fields from radiating components in the package, such as inductors and transmission lines [8], [9].

Metals create shielding purely from EMI absorption.

However, to compensate for the disadvantages of traditional metals such as their susceptibility to corrosion and heavy weight, researchers have recently investigated graphene sheets as a replacement for conventional metal shields [2], [10]. Since the thickness of monolayer graphene is 0.335 nm, ultra-thin multi-layer structures or composites with polymers, which can perform as a shield within miniaturized RF modules, can be created [11].

This paper explores graphene and multi-layered nanomagnetic structures to determine their effectiveness in EMI shielding, and compares them with copper. Section II analyzes the potential of graphene composites, discusses fabrication of graphene shields, and characterizes their shielding effectiveness. Section III discusses the analytical modeling of nanomagnetic materials and presents simulation results. After illustrating the fabrication process to form nanomagnetic multi-layers, their shielding effectiveness is characterized.

II. GRAPHENE EMI SHIELDING

Thin-film structures based on two-dimensional graphene sheets have been the focus of a number of studies because of their outstanding electrical and mechanical properties. The electrical conductivity of graphene is 2.62×10^2 S/m, while that of multi-walled carbon nanotubes is 5.43×10^2 S/m [12], [13]. Such high conductivity results in thin skin depth, leading to the decay of the electromagnetic field caused by absorption loss within the shielding material. Furthermore, since reflection loss at interfaces between any two materials is dependent on the difference between the characteristic impedance of the shield and surrounding material, a high electrical conductive material is required [14].

From the viewpoint of absorption and reflection losses, graphene may be an optimal shielding material. In addition, because of its mechanical properties, graphene has been considered a promising candidate as an EMI shield [15]. Compared to traditional metal shields, graphene itself is robust, lightweight, and flexible, so it has the potential for commercial applications [10].

To obtain higher shielding effectiveness with thinner

TABLE I
LIST OF GRAPHENE-BASED EMI SAMPLES

| Sample | Material Description |
|--------|---|
| A | 15 wt% (8.8 vol%) of functionalized graphene in epoxy |
| B | Graphene oxide film annealed at 2000 °C (8.4 μm) |
| C | Graphene oxide film annealed at 2000 °C (2.7 μm) |
| D | Mono-layer of graphene (MLG) papers produced in Acetone/DMF mixture |
| E | Annealed at 250 °C before the MLG process in Sample D |
| F | Mechanical compression added to Sample E |
| G | 60 vol% of MLG in polymer |
| H | 50 vol% of MLG in polymer |
| I | 30 vol% of MLG in polymer |
| J | GNP film produced by GNP concentration of 0.5 mg/ml |
| K | GNP film produced by GNP concentration of 1.0 mg/ml |
| L | Thermal annealing performed after the Sample K process |
| M | Mono-layer graphene on OHP film |

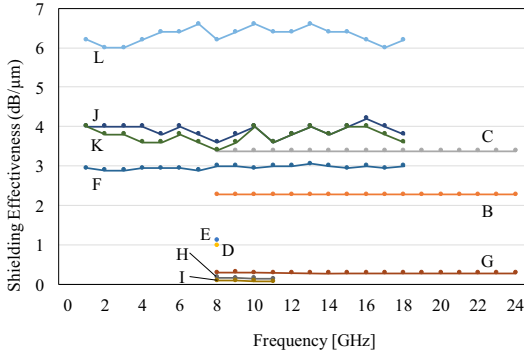


Figure 1. Shielding effectiveness comparison of Samples B-M.

graphene-included sheets, researchers have devoted considerable effort aimed at commercializing graphene EMI shielding. The normalized shielding effectiveness (per 1 micron) of different graphene composites are compared in Table I.

Polymeric composites with embedded graphene sheets maintain high electrical conductivity and more stable mechanical strength of samples (e.g. Sample A) [10]. Dispersing in polymers also reduced the production of graphene oxides (e.g., Sample G) [16]. It has been experimentally confirmed that polymeric thinfilms incorporated with graphene layers exhibit higher absorption loss and total shielding effectiveness, shown in Fig. 1 (i.e., Samples G, H, and I) [16].

In addition, the films fabricated by the spray deposition of the suspension of graphene nanoplatelets (GNPs) enable very thin EMI shields and enhance the shielding effectiveness of the structure. A higher concentration of GNPs does not necessarily increase shielding effectiveness because of the inefficiency of the exfoliation of the sonication process, resulting in the lower conductivity of the materials (i.e., Samples J and K) [15].

Furthermore, the mechanical compression of thinfilms (i.e., Sample F) provides lower porosity and higher conductivity than the sample without the compression

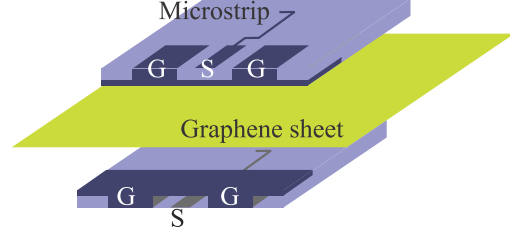


Figure 2. Characterization setup with microstrip structures for the shielding effectiveness (SE) measurement of graphene sheets. The signal pads (S) are placed between two ground pads (G).

(i.e., Samples D and E) [17]. This process offers higher reflection loss and lower absorption loss resulting from their thinner structures.

Another key method to increase shielding effectiveness of thinfilms, which is widely investigated nowadays, is to anneal the samples (i.e., Samples B and C) [18]. The shielding effectiveness measured after annealing is improved in all the cases, as listed in Table I, comparing Sample E with D, and L with J and K. Sample L has 2.5-dB higher shielding effectiveness than the non-annealed samples (e.g., Sample J) [15]. Moreover, taking advantage of the absorption property of graphene, Kim *et al.* [19] measured the reduction of the vertical noise coupling by the mono-layer graphene shield (i.e., Sample M) in the frequency range 2.5-7 GHz, where shielding effect of mono-layer graphene is verified between a DC-DC converter and a wideband LNA.

A. Fabrication of Graphene Shields

To characterize the shielding effectiveness of graphene sheets, GNPs are employed for fabrication. After GNPs are suspended with ethanol solvent, they are dip-coated on both sides of a polyethylene terephthalate (PET) substrate, which has 300 μm thickness. The fabricated graphene sheet has a total thickness of 4.24 μm .

B. Graphene Shielding Effectiveness Measurement Setup

For the measurement of the shielding effectiveness of the graphene sample, two microstrip structures are developed. Signals are transmitted from one of the two microstrips and received at the other microstrip as illustrated in Fig. 2. The graphene-sheet shield on PET is placed between the two microstrips. From the setup, S_{21} parameter, which stands for forward transmission, is measured using a vector network analyzer.

C. Characterization of Graphene Shields

In the EMI shielding theory, shielding effectiveness is defined as Eq. (1), and is plotted in Fig. 3 in the frequency range of 0.1 GHz to 8.4 GHz. The result (Fig. 3) shows that the shielding effectiveness of the graphene sample on PET is 46.0 dB, whereas PET sample showed 22.0 dB at 2.09 GHz. When the effect of the PET substrate is subtracted, the shielding effectiveness of the graphene sheet is 24.0 dB,

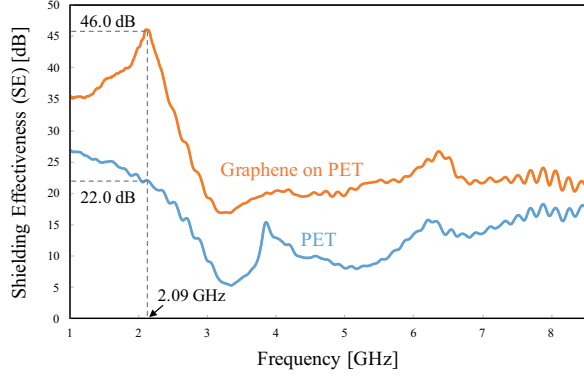


Figure 3. Shielding effectiveness measurement of graphene shields.

which means that the normalized shielding effectiveness (per micron) is $5.66 \text{ dB}/\mu\text{m}$. This value is higher than that of the samples shown previously in Fig. 1.

$$SE = -10 \log_{10} |S_{21}|^2 \quad (1)$$

Since the traditional shielding material, copper, shows $7.93 \text{ dB}/\mu\text{m}$ at 2.09 GHz, it is concluded that the shielding effectiveness per unit thickness is comparable to that of copper. In addition to its light weight and high robustness, graphene sheets fabricated through the simple dip-coating process can achieve $5.66 \text{ dB}/\mu\text{m}$.

III. NANOSTRUCTURED SHIELDS

Traditionally, EMI shielding has been implemented using metals such as copper, iron, and aluminum [14]. In addition to these conventional metals, shielding of magnetic field necessitates the use of magnetic materials because of their high impedance [20], [21]. Therefore, analytical simulation is performed based on fundamental field theories by comparing shielding effectiveness of each material, which is dependent on absorption loss, reflection loss, and multiple reflection. The design rules of simulation under consideration are tabulated in Table II. Through simulation, it is assumed that a thinfilm shield is placed between an EMI source and victim in the near field, and electromagnetic wave propagates vertically into the shield plane.

A. Synthesis of Multi-layered Metallic Nanostructures

Through analytical simulations, shielding effectiveness (SE) of three materials, which is defined by Eq. (1), is calculated to estimate an optimal material for shielding with the geometry discussed above. The shielding effectiveness of the ferromagnetic material, Nickel-Iron (NiFe) (i.e., Sample G), is compared with the conventional material copper (Cu) (i.e., Sample P). Furthermore, the shielding effectiveness of nanomagnetic multiple layers (i.e., Sample Q) is also examined. The primary advantage of such multi-layer shield is to shield electric field by interfering signals in a low-conductivity metallic layer that is sandwiched between two metallic layers having higher

TABLE II
DESIGN RULES

| Parameters | Dimensions |
|------------------------------------|------------------|
| Frequency range | 100 kHz - 10 MHz |
| Distance between Source and Shield | 2 cm |
| Shield thickness | $5 \mu\text{m}$ |

TABLE III
LIST OF METAL, FERROMAGNETIC, AND MULTI-LAYERED SAMPLES

| Sample Names | Material Composition | Thickness |
|--------------|--|-----------------|
| Sample P | Copper | $5 \mu\text{m}$ |
| Sample Q | $(0.3 \mu\text{m NiFe} + 0.7 \mu\text{m Cu}) \times 5$ | $5 \mu\text{m}$ |
| Sample R | NiFe | $5 \mu\text{m}$ |

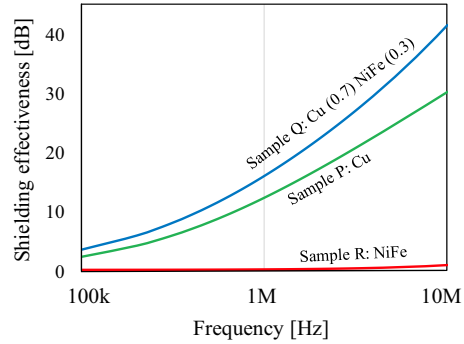


Figure 4. Shielding effectiveness simulation of metal, ferromagnetic, and multi-layered samples.

conductivity. Namely, it is expected that internal reflection enhances its total shielding effectiveness in case of Sample Q.

The comparison of shielding effectiveness of each material listed in Table III is shown in Fig. 4. The multi-layered nanomagnetic structure (Sample Q) shows higher shielding effectiveness than those of pure Cu and NiFe blanket films. These simulation results illustrate that difference in impedances at the interface of two layers improves total shielding effectiveness since internal reflection occurs in a multi-layer structure.

B. Characterization Setup for Nanomagnetic Laminates

To characterize the shielding effectiveness of the three samples shown in Table III, two measurement topologies are developed. One is the setup where magnetic field penetrates a shield perpendicularly as shown in Fig. 5 (a). On the other hand, a thinfilm shown in the Fig. 5 (b) acts as a lateral or tangential shield. The distance of a coil to the other coil is set to be 2 cm in case of the vertical shield (Fig. 5 (a)), and 4 cm in the lateral-shield case (Fig. 5 (b)).

C. Fabrication of Nanomagnetic Laminates

To characterize the shielding effectiveness of the materials discussed in Section III B, the samples P and Q shown in Table III are fabricated, using the design rules in Table II. Sputtering deposition is employed to synthesize the two

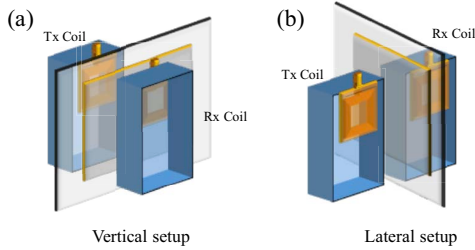


Figure 5. Characterization setups to measure the S_{21} parameter of (a) vertical and (b) lateral noise coupling.

structures: the 5 m Cu blanket film (Sample P) and multi-layered structure (Sample Q). These thinfilms are deposited on biaxially-oriented polyethylene films, which do not affect their shielding effectiveness.

D. Shielding Effectiveness Measurement of Metallic Materials

Shielding effectiveness of the materials shown in Table III is measured using the setups shown in Fig. 5. The shielding effectiveness is plotted in the frequency range of 500 kHz to 10 MHz (Fig. 6 (a) and (b)). Fig. 6 (a) demonstrates that pure Cu (Sample P) shows better shielding effectiveness than that of copper in the whole frequency range. The conventional material Cu can still reduce vertical noise coupling in 3D mixed-signal systems more efficiently than the multi-layered structures.

For the lateral magnetic shielding case, Cu(0.7)-NiFe(0.3) stack (Sample Q) had higher shielding effectiveness than Cu blanket film (Sample P) in the frequency range from 800 kHz to 10 MHz. However, the shielding effectiveness of nanomagnetic multi-layers (Sample Q) is no longer higher than that of the pure copper above 10 MHz. Especially, the shielding effectiveness of Cu(0.7)-NiFe(0.3) stack is 3.24 dB higher than that of copper at 2 MHz, representing the high switching frequency for power management ICs. From the measurements of tangential magnetic field shielding, the multi-layered nanomagnetic structures are more effective than the traditional material copper at 2 MHz; therefore, the structures can contribute to the better performance of high switching frequency power management ICs for automotive safety applications.

IV. CONCLUSION

This paper demonstrated miniaturized and integrated EMI shielding nanostructures for component-level EMI isolation and external EMI shielding in ultra-miniaturized IoT and wearable systems. Graphene nanocomposites, multi-layered nanomagnetic and copper shielding materials were modeled, designed, synthesized and characterized for their shielding effectiveness.

Graphene films showed $5.66 \text{ dB}/\mu\text{m}$ shielding effectiveness, comparable to that of copper, but with much simpler dip-coating process. Nanomagnetic multi-layers were designed, modeled and characterized for their shielding effectiveness

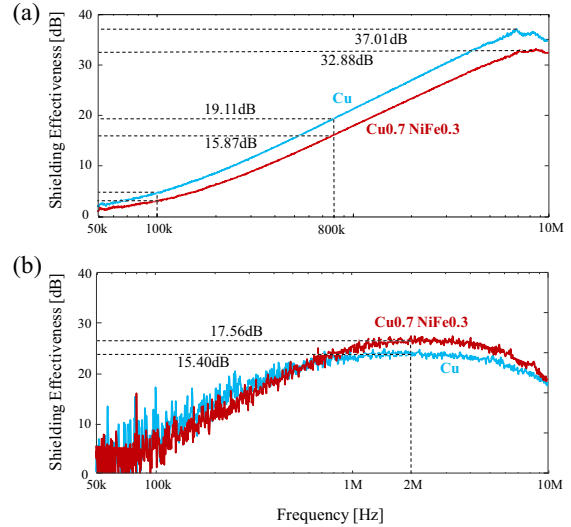


Figure 6. Shielding effectiveness measurement of Cu, NiFe, and multi-layered structures.

in the second part of the work. Results indicated that the structure had better shielding effectiveness than that of copper for tangential magnetic fields.

ACKNOWLEDGMENT

The authors wish to acknowledge Dr. Srikrishna Sitaraman for help with his advice, and Dr. Himani Sharma for help with the fabrication of graphene samples. Additionally, they would like to thank the industry sponsors of the consortia program at GT-PRC for their technical guidance and support.

REFERENCES

- [1] C. Banyai and D. Gerke, *EMI Design Techniques for Microcontrollers in Automotive Applications*, no. 272673, 1996.
- [2] N. Karim, Improving electromagnetic compatibility performance of packages and SiP modules using a conformal shielding solution, *2010 Asia-Pacific Int. Symp. Electromagn. Compat.*, pp. 5659, 2010.
- [3] A. Martin, AN-2162 Simple Success With Conducted EMI From DC-DC Converters, no. November 2011, pp. 113, 2013.
- [4] R. Minami, J. Hong, D. Imanishi, K. Okada, and A. Matsuzawa, Measurement of Integrated PA-to-LNA Isolation on Si CMOS Chip, 2010.
- [5] K. Matsuge, S. Himura, M. Ishida, T. Kitahara, and T. Yamamoto, Full RF Module with Embedded Filters for 2.4GHz and 5GHz Dual Band WLAN Applications, pp. 629632, 2004.
- [6] C. Y. Hsiao, C. H. Huang, C. De Wang, K. H. Liao, C. H. Shen, C. C. Wang, and T. L. Wu, Mold-based compartment shielding to mitigate the intra-system coupled noise on SiP modules, *IEEE Int. Symp. Electromagn. Compat.*, pp. 341344, 2011.
- [7] S. Sitaraman, J. Min, M. R. Pulugurtha, M. S. Kim, V. Sundaram, and R. Tummala, Modeling, design and demonstration of integrated electromagnetic shielding for miniaturized RF SOP glass packages, 2015, pp. 19561960.
- [8] J. Pak, M. Ha, J. Kim, D. Kang, H. Choi, S. Kwon, K. La, and J. Kim, Focusing RFsinlHnddgia, 2008.
- [9] A. Suintives, A. Khajooeizadeh, and R. Abhari, Using Via Fences for Crosstalk Reduction in PCB Circuits, vol. 2, no. c, pp. 3437, 2006.
- [10] J. Liang, Y. Wang, Y. Huang, Y. Ma, Z. Liu, and J. Cai, Letter to the Editor Electromagnetic interference shielding of graphene / epoxy composites, *Carbon N. Y.*, vol. 47, no. 3, pp. 922925, 2008.

- [11] C. Lee, X. Wei, J. W. Kysar, and J. Hone, of Monolayer Graphene, vol. 321, no. July, pp. 385389, 2008.
- [12] B. Marinho, M. Ghislandi, E. Tkalya, C. E. Koning, and G. De With, Electrical conductivity of compacts of graphene , multi-wall carbon nanotubes , carbon black , and graphite powder, *Powder Technol.*, vol. 221, pp. 351358, 2012.
- [13] V. Eswaraiah, Electromagnetic interference (EMI) shielding of carbon nanostructured films, no. Iccce, pp. 150152, 2010.
- [14] Henrt W. Ott, *Electromagnetic Compatibility Engineering*. John Wiley & Sons, 2011.
- [15] C. Acquarelli, a Rinaldi, a Tamburrano, G. De Bellis, a G. D. Aloia, and M. S. Sarto, Graphene-based EMI shield obtained via spray deposition technique, pp. 488493, 2014.
- [16] W. Song, M. Cao, M. Lu, S. Bi, and C. Wang, Flexible graphene / polymer composite films in sandwich structures for effective electromagnetic interference shielding, *Carbon N. Y.*, vol. 66, pp. 6776, 2013.
- [17] L. Paliotta, G. De Bellis, A. Tamburrano, S. K. Balijepalli, S. Kaciulis, M. S. Sarto, F. Marra, and A. Rinaldi, Highly conductive multilayer-graphene paper as a flexible lightweight electromagnetic shield, *Carbon N. Y.*, vol. 89, pp. 260271, 2015.
- [18] B. Shen, B. Shen, W. Zhai, and W. Zheng, Ultrathin Flexible Graphene Film: An Excellent Thermal Conducting Material with Efficient EMI Shielding Ultrathin Flexible Graphene Film: An Excellent Thermal Conducting Material with Efficient EMI Shielding, no. February 2016, 2014.
- [19] K. Kim, K. Koo, S. Hong, J. Kim, B. Cho, and J. Kim, Graphene-based EMI shielding for vertical noise coupling reduction in 3D mixed-signal system, *2012 IEEE 21st Conf. Electr. Perform. Electron. Packag. Syst.*, pp. 145148, 2012.
- [20] P. M. Raj, D. Mishra, S. Sitaraman, and R. Tummala, Materials NanoScience Nanomagnetic Thinfilms for Advanced Inductors and EMI Shields in Smart Systems, *J. Mater. Nanosci.*, vol. 1, no. 1, pp. 3138, 2014.
- [21] K. Yamada, M. Ishida, S. Yutaka, and M. Yamaguchi, High-performance laminated thin-film shield with conductors and magnetic material multi-layer, *IEEE Int. Symp. Electromagn. Compat.*, vol. 1, pp. 432437, 2011.